PAPER

Development, construction and tests of the Mu2e electromagnetic calorimeter mechanical structures

Published by IOP Publishing for Sissa Medialab

Received: *September 29, 2021*
Revised: *November 2, 2021*
Accepted: *November 14, 2021*
Published: *January 5, 2022*

22nd International Workshop on Radiation Imaging Detectors
June 27–July 1, 2021
Ghent, Belgium

Development, construction and tests of the Mu2e electromagnetic calorimeter mechanical structures

N. Atanov,[a] V. Baranov,[a] L. Borrel,[b] C. Bloise,[c] J. Budagov,[a] S. Ceravolo,[c] F. Cervelli,[d] F. Colao,[e] M. Cordelli,[c] G. Corradi,[c] Y.I. Davydov,[a] S. Di Falco,[d] E. Diociaiuti,[c] S. Donati,[d,f] R. Donghia,[c] B. Echenard,[b] C. Ferrari,[d] A. Gioiosa,[d] S. Giovannella,[c] V. Giusti,[d] V. Glagolev,[a] F. Grancagnolo,[g] D. Hampai,[c] F. Happacher,[c] D. Hitlin,[b] D. Lin,[b] A. Marini,[d] M. Martini,[c,h] S. Middleton,[b] S. Miscetti,[c] L. Morescalchi,[d] D. Pasciuto,[d,f,*] E. Pedreschi,[d] F. Porter,[b] F. Raffaelli,[d] A. Saputi,[c] I. Sarra,[c] F. Spinella,[d] A. Taffara,[d] G.F. Tassielli,[g] V. Tereshchenko,[a] Z. Usubov,[a] I.I. Vasilyev,[a] A. Zanetti[i] and R.Y. Zhu[b] on behalf of the Mu2e collaboration

[a] *Joint Institute for Nuclear Research, Dubna, Russia*
[b] *California Institute of Technology, Pasadena, California, United States*
[c] *Laboratori Nazionali di Frascati dell'INFN, Frascati, Italy*
[d] *INFN — Sezione di Pisa, Pisa, Italy*
[e] *ENEA — Frascati, Frascati, Italy*
[f] *Department of Physics, University of Pisa, Pisa, Italy*
[g] *INFN — Sezione di Lecce, Lecce, Italy*
[h] *Department of Engineering Sciences, Guglielmo Marconi University, Rome, Italy*
[i] *INFN — Sezione di Trieste, Trieste, Italy*

E-mail: daniele.pasciuto@pi.infn.it

Abstract: The "muon-to-electron conversion" (Mu2e) experiment at Fermilab will search for the charged lepton flavour violating neutrino-less coherent conversion of a muon into an electron in the field of an aluminum nucleus. The observation of this process would be the unambiguous evidence of the existence of physics beyond the standard model. Mu2e detectors comprise a straw-tracker, an electromagnetic calorimeter and an external veto for cosmic rays. In particular, the calorimeter provides excellent electron identification, a fast calorimetric online trigger, and

*Corresponding author.

https://doi.org/10.1088/1748-0221/17/01/C01007

complementary information to aid pattern recognition and track reconstruction. The detector has been designed as a state-of-the-art crystal calorimeter and employs 1348 pure Cesium Iodide (CsI) crystals readout by UV-extended silicon photosensors and fast front-end and digitization electronics. A design consisting of two identical annular matrices (named "disks") positioned at the relative distance of 70 cm downstream the aluminum target along the muon beamline satisfies the Mu2e physics requirements. The hostile Mu2e operational conditions, in terms of radiation levels (total expected ionizing dose of 12 krad and a neutron fluence of 5×10^{10} n/cm^2 @ 1 MeV$_{\text{eq}}$ (Si)/y), magnetic field intensity (1 T) and vacuum level (10^{-4} Torr) have posed tight constraints on scintillating materials, sensors, electronics and on the design of the detector mechanical structures and material choice. The support structure of each 674 crystal matrix is composed of an aluminum hollow ring and parts made of open-cell vacuum-compatible carbon fiber. The photosensors and front-end electronics for the readout of each crystal are inserted in a machined copper holder and make a unique mechanical unit. The resulting 674 mechanical units are supported by a machined plate of vacuum-compatible plastic material. The plate also integrates the cooling system made of a network of copper lines flowing a low temperature radiation-hard fluid and placed in thermal contact with the copper holders to constitute a low resistance thermal bridge. The data acquisition electronics are hosted in aluminum custom crates positioned on the external lateral surface of the disks. The crates also integrate the electronics cooling system as lines running in parallel to the front-end system. In this paper we report on the calorimeter mechanical structure design, the mechanical and thermal simulations that have determined the design technological choices, and the status of component production, quality assurance tests and plans for assembly at Fermilab.

KEYWORDS: Detector design and construction technologies and materials; Manufacturing; Overall mechanics design (support structures and materials, vibration analysis etc.); Detector cooling and thermo-stabilization

2022 JINST 17 C01007

Contents

1 Introduction

The Mu2e experiment at Fermilab [1] will search for the Charged Lepton Flavor Violating (CLFV) neutrino-less, coherent conversion of a muon into an electron in the field of an aluminum nucleus. The experimental signature is a mono-energetic electron with an energy equal to the muon rest mass minus the corrections due to the nuclear recoil and the binding energy. For the aluminum nucleus, the energy of the mono-energetic electron is approximately 105 MeV. The layout of the Mu2e experiment at Fermilab is thoroughly described in [1]. A system of three superconductive solenoids produces and transports a high intensity pulsed muon beam to the aluminum target, where muons stop and form muonic atoms. The goal of the Mu2e detectors is detecting the conversion electron from the overwhelming background of particles originated from the standard physics processes which involve the muonic atoms.

2 The Mu2e calorimeter

The main detectors employed by Mu2e are a straw-tube tracker [2] and an electromagnetic calorimeter [3] located inside a vessel with a 10^{-4} Torr vacuum level, and surrounded by a large superconducting solenoid which generates an axial magnetic field of 1 T. The main calorimeter function is providing complementary information to the tracker to achieve a powerful μ/e separation which is crucial to extract the conversion electron signal from the expected overwhelming background [4]. The calorimeter is also exploited in a calorimeter-seeded track finder algorithm which improves track reconstruction efficiency and makes the algorithm more robust in high detector occupancy conditions. Moreover, the calorimeter is used to implement a fast online standalone

2022 JINST 17 C01007

trigger independent from the tracker. These tasks translate into the following requirements for 105 MeV electrons: (a) large geometric acceptance; (b) time resolution better than 500 ps; (c) energy resolution better than 10% and (d) position resolution of the order of 1 cm. The calorimeter has been designed to maintain a full functionality in the Mu2e very harsh operational conditions: 10^{-4} Torr vacuum level, 1 T magnetic field, and a very intense particle flux. Depending on the position, a maximum of Total Ionizing Dose (TID) of the order of 100 krad/year and a neutron fluence of the order of 10^{12} n_{eq}/cm^2 are expected over five years of data taking. Since the detectors will be accessible for maintenance on average only once per year, each calorimeter component is required to be highly reliable. The presence of the magnetic field requires the use of Silicon PhotoMultipliers (SiPMs) as photosensors. The required light collection, quantified by Monte Carlo simulation, is at least 20 photo-electrons (p.e.)/MeV. To have a redundant system, each crystal is readout by two photosensors that collect the light independently. After a long R & D program [5, 6], such requirements pushed the experiment to adopt a calorimeter made of undoped CsI crystals optically coupled to 14×20 mm^2 large area UV-extended SiPMs. A large SiPM + front-end boards matrix is embedded in the back plate that also integrates a network of cooling lines to control SiPM and front-end electronics temperature. The DAQ boards are hosted in a battery of 10 crates/disk placed on the disk lateral surface.

The final calorimeter design (figure 1) consists of two disks, each containing a matrix of undoped CsI crystals that are coupled to two SiPMs each. The distance between the two disks is 700 mm to maximize the acceptance for the 105 MeV signal electrons following a helical trajectory in the solenoidal magnetic field. A fluorin-rich liquid activated by a neutron generator is fluxed through a network of pipes housed in the frontal source plate to provide the absolute energy scale and the response equalization among the crystals. A laser system is used to monitor and calibrate SiPM gains each 1.4 s obtaining an equalization of 0.5%, using fibers enlightening directly each single crystal/SiPM with the same amount of light.

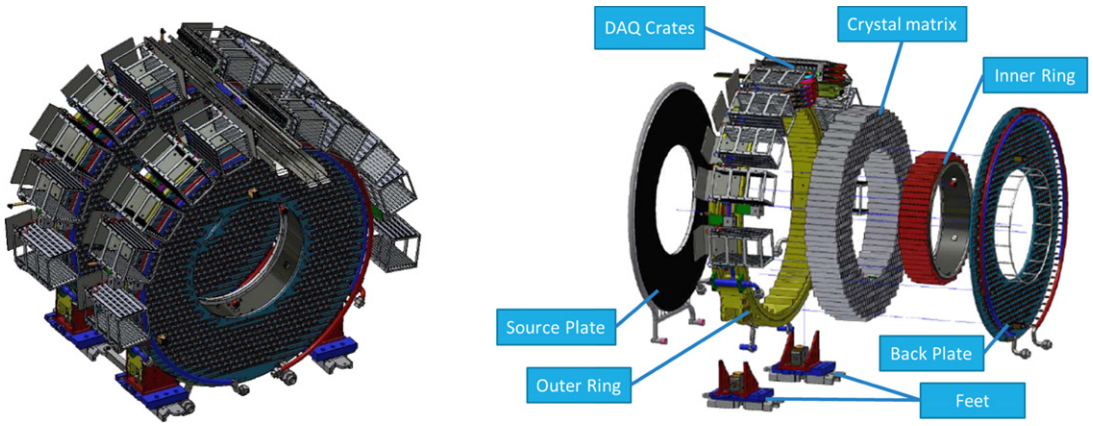

Figure 1. CAD drawings of the Mu2e electromagnetic calorimeter. Global view of the two disks (left). Exploded view of one disk: the outer ring, the source plate, the crystal matrix, the DAQ crates, the inner ring, the back plate and the feet are shown (right).

2022 JINST 17 C01007

3 The matrix of CsI crystals and the outer ring

The heart of each disk is the ring-shaped matrix of 674 un-doped CsI crystals ($34 \times 34 \times 200$ mm^3) which has an internal/external diameter of 650 mm/1314 mm. Crystals are wrapped in Tyvek foils (150 μm thick) to improve internal light reflection and separated vertically and horizontally with black Tedlar foils (50 μm thick) to minimize optical cross-talk.

The crystal quality control procedure was organized as follows: a batch of 60 crystals was shipped from each producer (Saint-Gobain, France and SICCAS, China) and received at the Fermilab Shipping and Receiving office and then sent to the Mu2e Calorimeter Laboratory at SiDet, Lab A [7, 8]. Here, a visual survey excluded the presence of large defects such as large notches, dents, scratches or bubbles. Then, the mechanical specifications [9] were checked with a Coordinate Measuring Machine (CMM) model: Brown & Sharpe Global Image 9-15-8. The crystals that did not satisfy the mechanical requirements were rejected and sent back to the producer. Figure 2 shows the dimensional survey results. The accepted crystals were wrapped and the measurements of the optical properties and Radiation Induced Noise (RIN) were performed [10]. Finally, the crystals were placed in drawers where N_2 was flown to keep the crystals in a humidity free and controlled environment. Radiation hardness tests were carried out on a small randomly selected sample in Caltech, Pasadena (U.S.A.) [11, 12].

Since crystals are wrapped in Tyvek foils and separated by Tedlar foils, the total envelope of each crystal is uncertain (tenths of millimeter). We thus performed a series of vertical/horizontal crystals stacking tests (figure 3 left and center). The output was the crystals show an envelope larger than expected because of the multiple material layers used, and a tilting effect which increase with the height of the stacking column [9]. A model to predict where crystal (i, j) will be located in the donut-shaped matrix is thus be realized to have a more precise machining of inner/outer ring steps and SiPM module hollows in the backplate. For maximum flexibility, the inner/outer rings embed tools for a residual fine-tuning of the crystal positions and alignment with respect to the SiPMs matrix.

The crystal matrix is externally supported by the outer ring (figure 3 right) milled from a bulk block of Al6082 aluminum to maximize stiffness. The outer diameter and the thickness of the ring are 1460 mm and 146 mm, respectively. The lateral steps are spaced to accommodate and align the crystals rows. A FEM analysis has been performed considering the weight of the crystal matrix, pushing the inner surface and of the crates with the digitizing board, pushing the top surface. The disk leans isostatically on the two feet bulge structures. The maximum ring deformation, i.e. the vertical ring diameter variation, is of the order of 40 μm, which widely satisfies the calorimeter dimensional constraints. The outer ring also provides all the fastening features for the other components. It hosts the manifolds for the crate cooling system and supports the DAQ crates on the lateral surface. The outer ring will be inserted in an outer steel frame to transport the calorimeter from the Sidet Laboratory (where the assembly will take place), to the Mu2e experimental site. The two outer rings have been manufactured, and quality controlled. One ring has already been shipped to Fermilab and is ready for detector assembly while the other one is at INFN National Laboratory of Frascati to test the assembly procedures.

2022 JINST 17 C01007

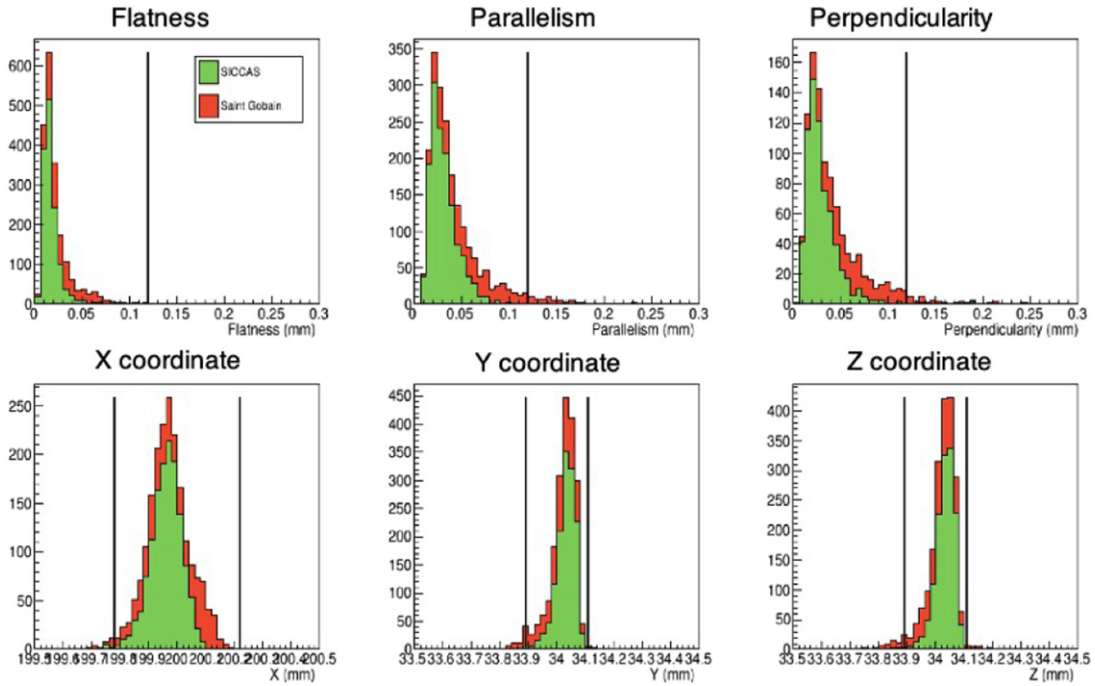

Figure 2. Results of the dimensional quality assurance tests of the production CsI crystals (measurements performed with a CMM at Fermilab). Flatness (top left), parallelism (top center) and perpendicularity (top right) and the X (bottom left), Y (bottom center) and Z (bottom right) dimensions for crystals produced by SICCAS (*green*) and Saint Gobain (*red*). The black vertical lines represent the specification requirements.

Figure 3. Exploded model of crystal wrapping (left). Crystal staggered tower during measurement (center). The outer ring during the quality assessment at Cerasa Mechanics (Perugia — Italy) (right).

4 Composite materials: the source plate and the inner ring

The material choice and budget of the mechanical structures that can be traversed by the particles have been optimized to minimize particle energy losses. The two components placed on the particle trajectories are the source panel, which is the frontal cover of the each crystal matrix, and

2022 JINST 17 C01007

the inner ring, which occupies the inner bore surface. They are both made of carbon fiber planes strengthened by light aluminum structures when necessary.

The source plate (figure 4 left) supports 10 thin-wall (0.375″ OD × 0.02″ thickness) aluminum tubes symmetrically arranged on each disk to flow the calibration source fluid (CF-770). It also provides the frontal enclosure for crystal protection. The source plate is made of a sandwich with 1.4 mm carbon fiber skins and a core of aluminum honeycomb (series 3003) 22 mm thick, 3/8″ cell size, and 0.003″ wall thickness. The expected energy loss is 1.2 MeV for 100 MeV electrons, which is still deemed compatible with Mu2e physics reach [13].

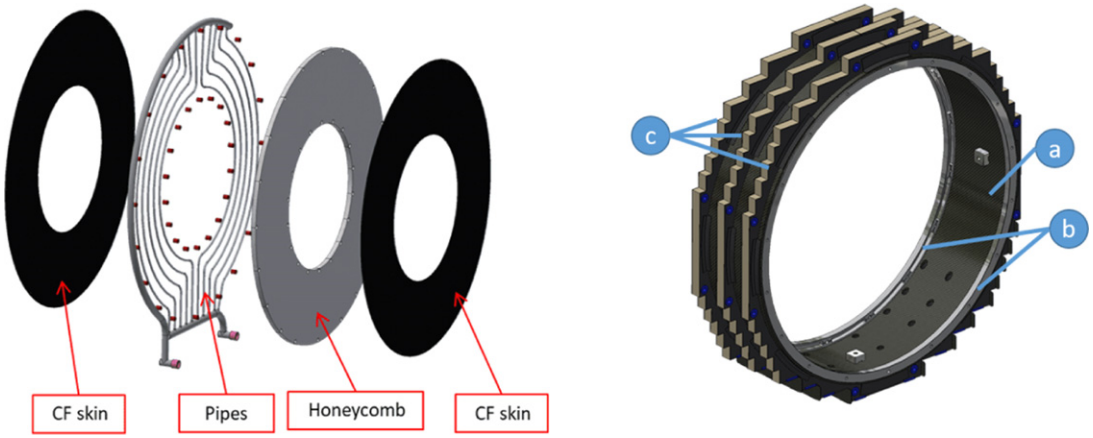

Figure 4. Exploded model of the source plate (left) and inner ring (right).

The inner ring (figure 4 right) performs a fundamental function for the support and alignment of the crystal matrix. It is made of:

- A carbon fiber cylindrical skin with an internal diameter of 712 mm, 4.2 mm thick, an F-.220/193/50 CF fabric (0/90° texture) with cyanate ester resin;
- Two 5083 H111 aluminum alloy reinforcement internal rings with an internal diameter of 672 mm, an outer diameter of 712 mm, 13 mm thick to increase its stiffness;
- Three outer step ribs made of a sandwich slab with 1.4 mm carbon fiber skins (same as the cylindrical skin) and a core of aluminum honeycomb (series 3003) 22 mm thick, 3/8″ cell size, and 0.003″ wall thickness.

The inner ring is connected and supported by the back plate and source plate and provides the internal vertical/horizontal reference for the crystal matrix. The inner ring also embeds mobile feet which allow to adjust its position and improve the precision of crystal alignment.

5 Plastic materials: the back plate

The back plate is the rear mechanical enclosure of the calorimeter. It also supports the 674 front-end units which include the SiPMs and front-end electronic boards. The SiPM and front-end

2022 JINST 17 C01007

electronic modules are composed of 2 SiPMs glued on a copper holder, 2 front-end boards and a copper protective cage (figure 5). The modules are fastened directly on the back plate cooling lines to optimize thermal conductivity. The back plate is made of a milled PEEK plate (20 mm thick) built by gluing 2 smaller plates with a V-notch joint because of the limited commercial. PEEK was chosen to optimize thermal isolation of the electronics and for its good outgassing characteristics.

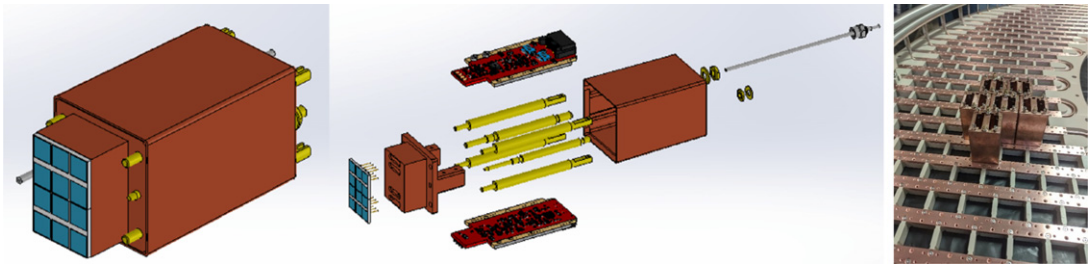

Figure 5. CAD model of a SiPM and front end electronics holder module (left and center). Some prototype modules mounted on the back plate (right).

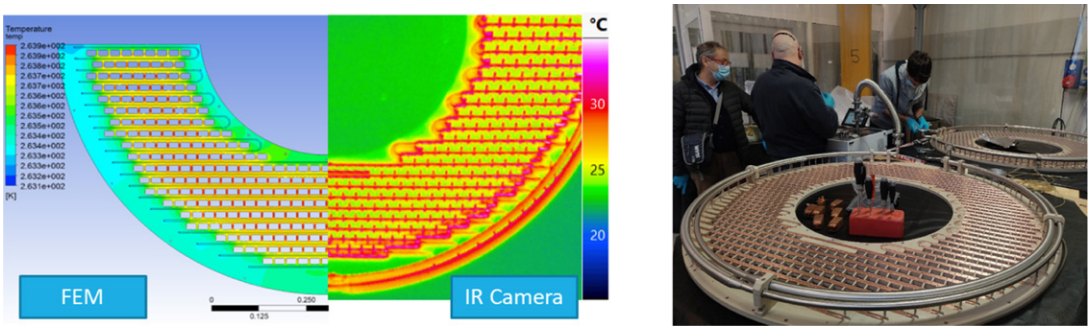

Figure 6. Thermal simulation of the back plate and test to check temperature homogeneity (left). Back plate leak tests performed at Cinel (Vigonza — Italy) after manufacturing and assembly (right).

The back plate integrates the cooling system of the front-end units. It embeds a network of vacuum brazed copper lines flowing fluid (3M Novec 649) at −15 °C to minimize SiPM dark current and mantain an acceptable signal/noise ratio over the three years of data taking. Two stainless steel (AISI 316L) I/O manifolds placed on the external border distribute the cooling fluid among the network of 38 parallel copper cooling lines embedded in the PEEK to maximize the temperature uniformity [14]. Tests to verify temperature uniformity have been performed at INFN Laboratories in Pisa by flowing HFE at 50 °C (figure 6 left). In the same Laboratory a geometrical and dimensional survey has been performed on a gantry shaped Coordinate Measuring Machine (DEA) as part of the quality control process. Leak tests have been performed at the manufacturer site in Vigonza (Italy) where a leak rate below 10^{-10} atm cc/s has been registered (figure 6 right).

2022 JINST 17 C01007

6 DAQ boards and crates

Each calorimeter disk supports 10 DAQ crates placed on its lateral surface to host 80 DAQ boards (Digitizer ReAdout Controller (DIRAC) [15] and Mezzanine, figure 7 left) which digitize and transmit the data received from the front-end through optical fibers out of the vessel to the central DAQ system. Each crate integrates a network of cooling lines to remove the 320 W dissipated by the set of 8 DAQ boards. To reduce envelopes and optimize the system performance, the cooling lines are directly carved in the crate sides. Optimal thermal contact between the electronic components and the heat sink is achieved through a machined copper plate positioned on top of the DAQ boards and placed in thermal contact with the components with vacuum proof thermal grease (Apiezon). The DAQ crate structure (figure 7 right) is completed by a set of tungsten plates which protect the electronic components from the high level of radiation present in experimental area at run time. Thermal simulations and experimental tests have been performed in air as well as in vacuum to crosscheck the cooling system performance [16]. The DAQ crates production is now progressing.

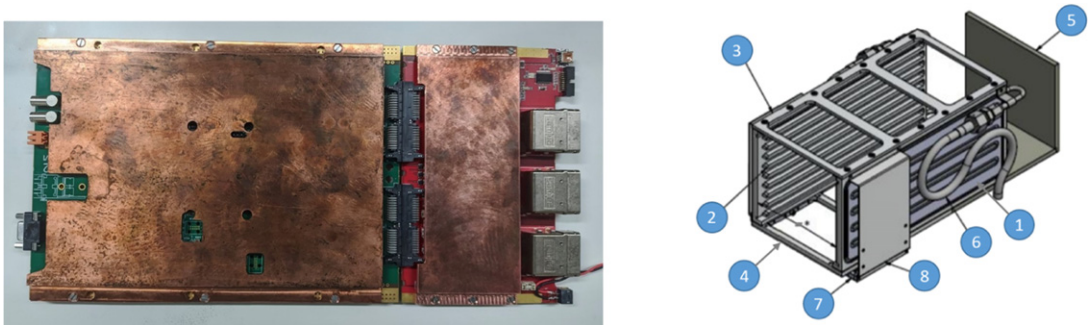

Figure 7. DAQ boards with the copper shield: the Dirac (*green*) and the Mezzanine (*red*) (left). CAD Model of the DAQ crate: external side (1), internal side (2), top (3), bottom (4), tungsten shield (5), inlet/outlet pipe (6), cable holder (7), cable containment wall (8) (right).

7 Plans for detector assembly

The calorimeter will be assembled in a 10000-class cleanroom built in the SiDet Laboratory at Fermilab (figure 8 left). Two assembly stations will be available to test the first assembled disk while building the second one. An assembly station has been realized also at the INFN National Laboratory of Frascati to test the components received from the vendors before shipment to Fermilab (figure 8 right). Outgassing tests of the components will be performed before assembly in dedicated vessels (the most critical components are crystals and cables) and the alignment of the crystal matrix will be continuously monitored during detector assembly. Tests of the cooling system and electronic components will be continuously performed during and after detector assembly.

2022 JINST 17 C01007

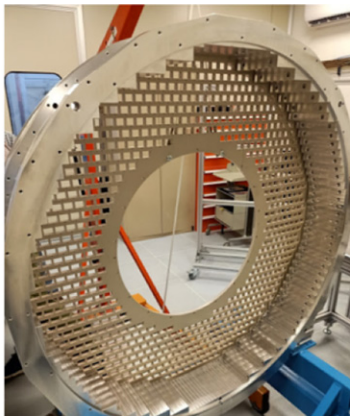

Figure 8. Photograph of the cleanroom for detector assembly at SiDet Laboratory — Fermilab (left). Photograph of the outer ring and back plate assembled at INFN National Laboratory of Frascati (right).

8 Conclusions

The design of the Mu2e electromagnetic calorimeter mechanical structures has been finalized after many years of research and development. At the time of writing this paper, most components have been built and are now being tested for quality assurance. The production and quality assurance of the cesium iodide crystals and silicon photomultipliers have been completed. The production of the front-end electronics has been completed, whereas data acquisition electronics is currently progressing. The detector assembly is expected to be completed in 2022.

Acknowledgments

We are grateful for the vital contributions of the Fermilab staff and the technical staff of the participating institutions. This work was supported by the U.S.A. Department of Energy; the Istituto Nazionale di Fisica Nucleare, Italy; the Science and Technology Facilities Council, U.K.; the Ministry of Education and Science, Russian Federation; the National Science Foundation, U.S.A.; the Thousand Talents Plan, China; the Helmholtz Association, Germany; and the EU Horizon 2020 Research and Innovation Program under the Marie Sklodowska-Curie Grant Agreement No. 690385, 734303, 822185, 858199, 101003460. This document was prepared by members of the Mu2e collaboration using the resources of the Fermi National Accelerator Laboratory (Fermilab), a U.S.A. Department of Energy, Office of Science, HEP User Facility. Fermilab is managed by Fermi Research Alliance, LLC (FRA), acting under Contract No. DE-AC02-07CH11359.

References

[1] L. Bartoszek et al., *Mu2e Technical Design Report* (2014), arXiv:1501.05241.

[2] The Mu2e collaboration, M. Lee, *The straw tube tracker for the Mu2e experiment, Nucl. Part. Phys. Proc.* **273** (2016) 2530.

2022 JINST 17 C01007

[3] N. Atanov et al., *The calorimeter of the Mu2e experiment at Fermilab,* 2017 *JINST* **12** C01061.

[4] N. Atanov et al., *Design and status of the Mu2e crystal calorimeter,* *IEEE Trans. Nucl. Sci.* **65** (2018) 2073.

[5] N. Atanov et al., *Measurement of time resolution of the Mu2e LYSO calorimeter prototype,* *Nucl. Instrum. Meth. A* **812** (2016) 104.

[6] O. Atanova et al., *Measurement of the energy and time resolution of a undoped CsI + MPPC array for the Mu2e experiment,* 2017 *JINST* **12** P05007.

[7] D. Pasciuto, *Calo QA Lab at SiDet, Info and documents*, Internal Report: Mu2eDoc16988.

[8] N. Atanov et al., *The Mu2e e.m. calorimeter: crystals and SiPMs production status,* *IEEE Trans. Nucl. Sci.* **67** (2020) 978.

[9] D. Pasciuto, *Physical and mechanical properties study of CsI scintillation crystals and design of the mechanical structure for the Mu2e electromagnetic calorimeter at Fermilab,* Ph.D. Thesis, Università degli studi Guglielmo Marconi (2020–2021).

[10] N. Atanova et al., *Quality assurance on undoped CsI crystals for the Mu2e experiment,* *IEEE Trans. Nucl. Sci.* **65** (2017) 752.

[11] E. Diociaiuti, *Study of the Mu2e sensitivity to the $\mu^- \rightarrow e^+$ conversion process,* Ph.D. Thesis, Università degli studi Tor Vergata (2019–2020).

[12] M. Cordelli et al., *Summary of CsI crystals production and related QA tests*, Internal Presentation: Mu2eDoc35564.

[13] N. Atanova et al., *The Mu2e calorimeter final technical design report, TDR*, arXiv:1802.06341 (2018).

[14] L. Morescalchi et al., *Automated test station for the characterization of custom silicon photomultipliers for the Mu2e calorimeter,* *PoS* **TWEPP2018** (2019) 017.

[15] E. Pedreschi et al., *The digitizer readout controller (DIRAC) of the Mu2e electromagnetic calorimeter at Fermilab,* *PoS* **TWEPP2019** (2020) 119.

[16] E. Benedetti, *Design and thermal analysis of the Mu2e experiment calorimeter,* Master Thesis, Università di Pisa (2017–2018).

2022 JINST 17 C01007